Biol Invasions (2010) 12:1543–1555
DOI 10.1007/s10530-009-9567-4

ORIGINAL PAPER

A multiscale model for plant invasion through allelopathic suppression

D. R. de Souza · M. L. Martins · F. M. S. Carmo

Received: 11 October 2008 / Accepted: 19 August 2009 / Published online: 18 September 2009

Abstract In the present paper, we propose and study by numerical simulations a multiscale model for plant invasion based on allelopathic suppression in a homogeneous environment. The negative effects on seed production and germination, establishment and mortality of native plants generated by the root-secreted alien phytotoxin constitute the basic mechanism contributing to invasiveness. We obtained the invasion patterns, their success probabilities, the time evolution of plant populations, the gyration radius and the border roughness of the invaded region. As an important result, it was observed that, in addition to the phytotoxin nature (synthesis and degradation rates, diffusivity and phytotoxic threshold), invasive patterns and invasion success depend on the kind of native plants present in the area. In fact, both success and invasion speed decrease in the presence of resistant native plants. Also, self-affine invasion fronts are smooth (Hurst exponent $H = 1$) in the absence of resistant plants, but are rough ($H \neq 1$) on the contrary. Furthermore, if the resistant native species are randomly distributed on the landscape, the invasion front exhibits long-range correlations ($H \sim 0.76$), while its border is anti-correlated ($H \sim 0.20$), if resistant plants are distributed in patches. Finally, the cluster size distribution functions of resistant plants are exponentials with characteristic cluster sizes increasing in time.

Keywords Allelopathy · Plant invasion · Multiscale modeling

D. R. de Souza · M. L. Martins (✉)
Departamento de Física, Universidade Federal de Viçosa, Viçosa, MG 36570-000, Brazil
e-mail: mmartins@ufv.br

Present Address:
D. R. de Souza
Instituto de Física, Universidade de São Paulo 05508-090, Cidade Universitária, São Paulo, SP, Brazil
e-mail: davidrs@if.usp.br

M. L. Martins
National Institute of Science and Technology for Complex Systems, Universidade Federal de Viçosa, Viçosa, MG 36570-000, Brazil

F. M. S. Carmo
Departamento de Biologia Geral, Universidade Federal de Viçosa, Viçosa, MG 36570-000, Brazil
e-mail: fmcarmo@ufv.br

Introduction

There is currently much interest in understanding biological invasions. This world-wide phenomenon represents a major threat for ecosystems functioning and biodiversity conservation, water availability, and agricultural production (Chou 1999; Dean 1998; Drake et al. 1989; Shigesada and Kawasaki 1997). Preventing biological invasions and predicting their spreading patterns emerge as imperative tasks in an

age focused on biotechnology. Indeed, issues concerning potential ecological or agronomic problems caused by genetically modified organisms provoke lively debates within the scientific community (Dale et al. 2002; Snow 2002) and touch complex socio-economic and ethical questions transcending the realms of science.

From the mathematical point of view, patterns of biological invasion are interesting examples of spontaneous symmetry breaking in complex systems. The spreading of an alien species from the place where it has been originally introduced in the habitat (local invasion) can progress in various ways. In a homogeneous environment invasion frequently generates smooth stationary traveling population waves (Petrovskii and Shigesada 2001). More complicated regimes in which the traveling fronts become transient or oscillatory before the formation of spatial patterns can be observed in a heterogeneous environment, or under the influence of other species (Sherratt et al. 1995; Shigesada et al. 1986).

The leading theory for exotic plant invasion is the escape of invader species from the pathogens and herbivores that regulate their population sizes in their original habitat, freeing them to focus their full potential on resource competition (Crawley 1996). Nevertheless, interspecific interactions between the invader and the native plants have rarely been considered (Cannas et al. 2003; Walker and Vitousek 1991). Recent results, however, indicate that some exotic invasive plants may use competitive mechanisms to disrupt inherent, coevolved interactions among long-associated native species constituting the communities they invade (Bais et al. 2002; Callaway and Aschehoug 2000).

One such mechanism is allelopathy, i.e., the suppression of germination or growth of neighboring plants by the release of toxic secondary chemical compounds. These secondary metabolites are leached, exuded or volatilized from the allelopathic plant into the environment (Rice 1984), acting as phytotoxins that contribute to the ecological stability of a plant community. However, if invasive species release a toxic compound and the individuals in the community lack resistance to it, the result may be the disruption of the existing plant community.

This seems to be the case with the Eurasian spotted knapweed (*Centaurea maculosa* Lam.) in the western United States (Bais et al. 2003; Callaway and Aschehoug 2000) and the *European Vulpia* spp. in Australia (An et al. 1996). *C. maculosa*, one of the most economically destructive plant invaders that have arrived in North America, releases the phytotoxin (−)-catechin from its roots which inhibits the germination and triggers the death of the root systems of native susceptible grass species (Bais et al. 2002, 2003).

In this paper we propose a multiscale mathematical model to investigate the dynamics of competing plant species in which one of them produces a phytotoxin affecting the others. It is assumed that the main factors contributing to invasiveness are the negative effects on native plants produced by a root-secreted alien phytotoxin. Among these effects are reduced seed production and germination, establishment and mortality of native plants. Several biological traits such as seed dispersion and germination, growth, death rate, characteristic resistance to allelochemicals, synthesis, dispersion and degradation of phytotoxins are taken into account. In section "Multiscale model" the multiscale approach is introduced. Section "Results" shows results from numerical simulations. In section "Discussion" our results are discussed. Finally, in section "Conclusion" some conclusions are drawn.

Multiscale model

Multiple scales in plant invasion

Plant invasions are intrinsically multiscale in nature. They involve phenomena occurring over a variety of spatial scales, ranging from geographic (e.g., regional extinctions of species) to molecular length scales (for example, use and break of metabolites by microbial communities). The relevant timescales vary from seconds for signaling events leading to cell death induced by a phytotoxin to tens of years for doubling times of invaded areas. Furthermore, all these processes and probably many others yet unknown, are strongly coupled. Indeed, the synthesis of a phtytotoxin may confer a competitive advantage to a given plant, increasing its abundance, altering microbial communities, nutrients and chemical mosaics in the soil. This, in turn, regulates the growth and spatial distribution of plants. To survive in a phytotoxic environment, plant species must have traits such as metabolic detoxification mechanisms that confer

resistance to phytotoxins and promote coexistence. Thus, information flows not only from the finer to coarser scales, but also between any scales.

The complexity of plant invasion through allelopathy manifests itself at least on three scales that may be distinguished and described in mathematical models: microscopic, mesoscopic and macroscopic (Bais et al. 2004). Specifically:

- The microscopic scale refers to molecular and sub-cellular phenomena occurring within the plant cell or at its plasma membrane. Examples are transcriptional events associated with phytotoxic response, dynamics of signaling cascades and/or metabolic pathways triggered by oxidative stress or defense purposes, fluxes of ions, protein secretion, and exudation of micro- and macromolecular metabolites by root border and epidermal cells etc. (Perry et al. 2005)
- The mesoscopic scale refers to physiological processes occurring in the rhizosphere or at plant level. Such processes include root-root and root-microbe communications, root colonization and growth, seed germination, waves of cell death along the roots, seedling mortality, reduced shoot differentiation, and inhibition of plant growth elicited by phytotoxins etc. (Perry et al. 2005; Varnijic et al. 2000).
- The macroscopic scale concerns processes occurring at the ecosystem level such as invasion fronts, convection and diffusion of nutrients and chemical compounds, seed dispersion, community integration and coevolution, chemical patterning of the soil etc. Here, a continuous approach is generally applied based on the assumption that there is a sufficiently large number of plants or molecules in order to define average continuous values for the macroscopic variables of interest across the whole environment.

Therefore, plant invasion, sometimes called the green cancer, is clearly a multiscale, non-linear dynamic problem as is tumor growth in multicellular organisms (Martins et al. 2007). The fundamental evolution of these problems can not be quantitatively described without the help of mathematical models. It sets up one of the major challenges of modern biology: to formulate models in which the rapidly increasing amount of information obtained at the various scales (from molecules to systems) is integrated in accurate models for use in prediction, control and simulations of the system response at the macroscopic description level. So, it is imperative to develop models able to capture the small scale effects on the large scales and provide the macroscopic responses of the systems accurately and efficiently without resolving the small scale details. In a multiscale approach, each scale of interest is described in terms of distinct physical models and all of them are coupled in a single model (Glimm and Sharp 1997; Krumhansl 2000). It is partially due to this coarse-grained description of the small scales that the resulting multiscale models become computationally more tractable.

Modeling the mesoscopic and macroscopic scales

A general, spatially explicit framework suitable to investigate invasion processes in ecological scales is based on cellular automata (CA) models (Ermentrout and Edelstein-Keshet 1993; Wolfram 1986). This approach provides more realistic theoretical population models incorporating spatial structure, non-linearity and stochasticity of the interactions, and the discrete, heterogeneous nature of the interacting organisms. This is particularly true for plant invasion and interspecific competition. Indeed, the effects of competition operate primarily on the individual, eventually affecting its reproduction, survival, dispersal, and niche use or habitat selection (Keddy 1989).

The present CA model relies on a fully age-structured representation of the individual plants, which disperse through seed germination in empty patches, compete for colonization of such empty sites, and die at a natural rate affected by the release of phytotoxins from the alien plant. The two-dimensional, non-stationary phytotoxin concentration field is computed based on a linear diffusive dynamics for these metabolites. Starting from an initial homogeneous environment of native plants in which a single invader specimen is introduced, the population dynamics generated from the collective history of each individual plant is observed.

The homogeneous environment is represented by a square lattice of $L \times L$ identical patches. Fixed, null boundary conditions simulating a closed system are used. Initially, all patches are occupied by the native species, except the center of the lattice invaded by an alien plant. Each patch or site has a size scale comparable to those of the plants' rhizosphere. Also,

the initial ages of plants are drawn stochastically with uniform probability in the range 1 to $t_{\max}$, the maximum longevity permitted. The following interaction rules define the CA evolution.

Plant reproduction

The plants can begin to disperse seeds at the age t_m corresponding to the onset of reproductive maturity. Mature plants produce seeds with a probability $p_s = (t_{\max} - t_m)^{-1}$, meaning that on average each one produces a seed crop along their life cycle. Every invader plant produces n_0 seeds, whereas native ones have their seed production affected by the local phytotoxin concentration F according to the expression

$$n_s = \begin{cases} n_0 e^{-a(F(\mathbf{x},t)-\theta)}, & \text{if } F(\mathbf{x},t) \geq \theta \\ n_0, & \text{otherwise.} \end{cases} \quad (1)$$

where n_s is the number of native seeds produced, a is a parameter measuring the phytotoxin inhibition of seed production and θ its concentration threshold for phytotoxity.

Growth (ageing) and death

At any time step an alien plant can die with a probability $p_d = 1-q$, in which q is the adult survival probability. For native plants the death probability is affected by the local phytotoxin concentration F as follows:

$$p_d = \begin{cases} 1 - q e^{-b[F(\mathbf{x},t)-\theta]}, & \text{if plant's age} \leq t_e \text{ and } F(\mathbf{x},t) \geq \theta \\ 1-q, & \text{otherwise.} \end{cases} \quad (2)$$

Here, the parameter b is a measure of the phytotoxin's efficiency to kill native plants. So, the model assumes that the mortality of young native plants (age $\leq t_e$, where t_e is the establishment time) is an increasing function of the local phytotoxin concentration, but it is unaffected for established plants (age $> t_e$). In the case of plant death, the corresponding site becomes empty and available for future colonization.

In turn, the value of q is calculated so that the probability that a plant survives up to $t_{\max}$ is smaller than 0.05 (Cannas et al. 2003). This probability is given by

$$P(t > t_{\max}) = 1 - \sum_{t=1}^{t_{\max}} (1-q) q^{t-1} = 1 - \frac{1 - q^{t_{\max}+1}}{q}. \quad (3)$$

The age of every surviving plant is increased by unit at each time step. Therefore, the model assumes that the natural survival probability q of native and invader species does not vary with age.

Dispersal and colonization

Mature plants (age $\geq$ t_m) can produce n_s seeds at each time step with a probability p_s. These seeds are dispersed through a neighborhood of radius $r_{\max}$, centered on the site of the parental plant, in accordance with the exponential distribution

$$n(r) = \frac{n_s}{1 + \sum_{r=1}^{r_{\max}} e^{-r/r_c}} e^{-r/r_c}. \quad (4)$$

Here, r_c is the characteristic length of seed dispersion. Distances are determined using the Manhattan metric ($d_{ij} = |x_i - x_j| + |y_i - y_j|$). So, the model assumes that seed dispersion is spatially isotropic in a two-dimensional lattice and uses a cutoff length $r_{\max}$ in order to truncate the exponential distribution for seed dispersion. The number $n(\mathbf{x}, t)$ of seeds present in every site decays at a rate γ_s after each time step. Thus, the parameter γ_s determines the seed viability in time. Finally, open boundary conditions, for which any site do not receive seeds from outside the lattice were used.

Seed germination occur only in empty sites with a fixed probability $p_g = p_0$ for the seeds of the alien plant, whereas their native counterparts germinate with a probability that decreases as the local phytotoxin concentration increases. Specifically, the probability of native seed germination is given by

$$p_g = \begin{cases} p_0 e^{-c[F(\mathbf{x},t)-\theta]}, & \text{if } F(\mathbf{x},t) \geq \theta \\ p_0, & \text{otherwise.} \end{cases} \quad (5)$$

Once germinated, native and alien species can colonize the empty site with a probability

$$p_c = 1 - (1 - p_g)^{n_{\text{seeds}}}, \quad (6)$$

where n_{seeds} is the total number of seeds of the corresponding species (native or invader) present in the site. The empty site will be colonized by the plant species having the greatest p_c value. If occasionally both native and alien plants have the same value of

p_c, then one of them is selected with equal chance and wins the competition.

Phytotoxin dynamics

The phytotoxins exuded from the roots of invader plants disperse through the soil. It is assumed in the present model that the phytotoxin concentration field $F(\mathbf{x}, t)$ is described by the diffusion equation

$$\frac{\partial F}{\partial t} = D\nabla^2 F + \sum_{\text{invader } i} \beta\delta(\mathbf{x} - \mathbf{x}_i(t)) - \gamma F. \quad (7)$$

This equation includes the simplest diffusive dynamics, the synthesis of the phytotoxin by the alien plants and its natural degradation in time as the only mechanisms involved in the spatio-temporal variation of the phytotoxin concentration. On the right hand side of this equation, the Laplacian term represents the Fick's diffusion which tends to equalize in space the phytotoxin concentration through its flux from regions of high concentrations to regions of low concentrations. In turn, the term containing a sum over Dirac delta functions $\delta(\mathbf{x}-\mathbf{x}_i(t))$ models the synthesis of phytotoxins by spatially localized sources (invader plants) at sites $\mathbf{x}_i$ in time t. At last, the third term on the right hand side of the equation represents the degradation of the phytotoxin in proportion to its local, instantaneous concentration. In Eq. 7, D is the diffusion constant of the phytotoxin and β and γ are its rates of synthesis and degradation, respectively. Thus, the γ term in this equation sets up a characteristic interaction distance between plants.

Dirichlet boundary conditions are imposed to the phytotoxin concentration field. The diffusion constant D, production and degradation rates, β and γ, respectively, are model parameters controlling phytotoxin dynamics. All of them are assumed to be constant in the model. Equation 7 is numerically solved through relaxational methods on a square lattice with a lattice unit equals to the radius of the plant rhizosphere.

Simulation protocol

The CA simulations were implemented through the following procedure: initially, a single invader plant with an age randomly chosen between t_m and $t_{\max}$ was introduced in the center of the lattice. At each time step (1) plants can die with probability p_d; (2) any survival plant ages and the mature ones can produce and disperse seeds with probability p_s; (3) the empty sites can be colonized, with probability p_c, by native or alien plants; (4) the non-stationary amount of phytotoxin is determined according to Eq. 7 for each lattice site; (5) the quantities of interest, namely, evolution in time of plant populations, gyration radius and roughness of the border of the invaded region, are determined. At the end of this sequence of actions, a new time step (Monte Carlo step-MCS) begins and the entire procedure is iterated.

In order to characterize the roughness of the border of an invasion pattern at each MCS, it was mapped into a radial profile containing the distances of all of its border sites to the mass center of the invaded region. This profile was generated as follows (Silva et al. 2006). Firstly, from the coordinates (x_i, y_i) of every site i at the invasion border, $i = 1,2,...,N$, the center of mass

$$x_{cm} = \frac{1}{N}\sum_{i=1}^{N} x_i \quad (8)$$

$$y_{cm} = \frac{1}{N}\sum_{i=1}^{N} y_i \quad (9)$$

is calculated. Secondly, the distance of every border site to the mass center, $r_i = \sqrt{(x_i - x_{cm})^2 + (y_i - y_{cm})^2}$, and its azimuthal angle $\theta_i = \arctan(x_i/y_i)$ were determined. So, the radial profile is given by the sequence of the distances r_i at the angle θ_i. The nature of the correlations in the radial profiles could be investigated through the analysis of the width W in the ε scale given by

$$W_N(\epsilon, t) = \frac{1}{N}\sum_{i=1}^{N} w_i(\epsilon, t), \quad (10)$$

with the local roughness $w_i(\epsilon, t)$ defined as

$$w_i(\epsilon, t) = \sqrt{\frac{1}{2\epsilon + 1}\sum_{j=i-\epsilon}^{i+\epsilon}\left[r(\theta_j, t) - \overline{r}_i(t)\right]^2}, \quad (11)$$

where $\overline{r}_i(t)$ is the mean radius on the interval $[\theta_{i-\epsilon}, \theta_{i+\epsilon}]$ centered on the angle θ_i. For self-affine profiles, the width W scales as a power law (Barabási and Stanley 1995)

$$W(\epsilon, t) \sim \epsilon^H. \quad (12)$$

The width W can distinguish two possible types of profiles. If the landscape is random, or even exhibits a finite correlation length extending up to a characteristic range (such as in Markov chains), $W \sim \epsilon^{1/2}$, as in a normal random walk. In contrast, if there is no characteristic length (infinitely long range correlations), then the width W scales as a power law

$$W(N) \sim \epsilon^H, \quad (13)$$

with the Hurst exponent $H \neq 1/2$. $H > 1/2$ implies that the profile presents persistent correlations, whereas $H < 1/2$ means antipersistent correlations, i.e., sequences of increasing radii are more likely to alternate with others in which the radii decrease.

Results

In order to investigate the controversial role of allelopathy in plant invasion, simulations were performed using basically the same values of the parameters for native and invader species. In this way, both native and alien plants have exactly the same skills in the competition for resources, if allelopathic suppression is neglected. Those values, listed in Table 1, were inspired in typical herb species with annual life cycle such as *Euphorbia heterophylla* L. Clearly, the natural spatial and temporal scales for the simulations are the size of a plant rhizosphere and a month, respectively. So, a MCS corresponds to 1 month and the lattice constant to about 10 cm, the typical radius of a grass rhizosphere. It is important to notice that the model parameters are rather arbitrary, since the details of most invasion processes are largely imprecise. This apparent handicap really represents the strength of the model's ability to investigate the dynamics of invasion in a broad range of parameter values.

The number of seeds produced by the alien plant, their maximum dispersion radius, the phytotoxic threshold of the phytotoxin secreted by the invader species, the fraction and spatial distribution of resistant plants in the native population were varied in the simulations. Figure 1a shows the invasion probability as a function of the ratio between the seed productions of invasive and native plants. In turn, the invasion probability as a function of the initial fraction of resistant plants in the native community is shown in Fig. 1b. Here, resistant plants have a phytotoxic threshold 100 times greater than the "normal" native plants. As expected, the chance of a successful invasion increases, if the alien plants produce more seeds than the native species. Also, the invasion probability decreases as the fraction of resistant plants increases in the native community. Finally, Fig. 1c, d show the invasion probability as a

Table 1 Parameters of the CA and their values used in the simulations

Parameter	Description	Hypothetical values (units)
$t_{\max}$	Plants' longevity	12 (months)
t_m	Age of reproductive maturity	3 (months)
t_e	Interval for plant establishment	2 (months)
n_0	Seeds/plant	100
$r_{\max}$	Maximum radius of seed dispersion	6 (lattice unit)
r_c	Characteristic length of seed dispersion	4 (lattice unit)
q	Adult survival probability	0.96
D	Phytotoxin diffusivity	1 ($cm^2\ h^{-1}$)
β	Phytotoxins release rate	0.5 (μg/week)
γ	Phytotoxin degradation rate	0.05 ($week^{-1}$)
θ	Phytotoxic concentration threshold	100 (μg/ml)
a	Inhibition of native seed production	0.20 (μg^{-1})
b	phytotoxic induced plant mortality	0.80 (μg^{-1})
c	Inhibition of native seed germination	0.40 (μg^{-1})
p_0	Germination probability	0.90
γ_s	Decay rate of viable seeds	0.05 ($week^{-1}$)

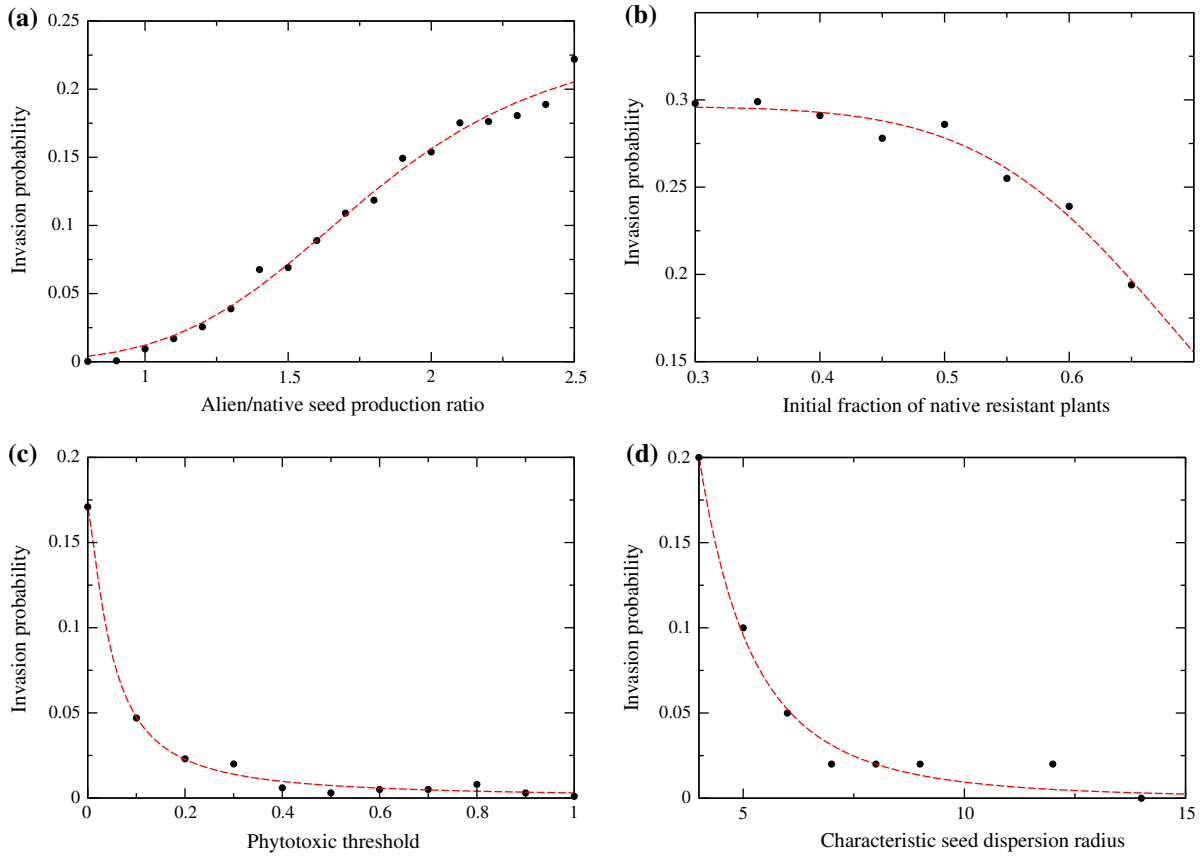

Fig. 1 Invasion probability as a function of **a** the ratio between the numbers of seeds produced by the invasive and the native plants, **b** the initial fraction of resistant plants, **c** the phytotoxic threshold, and **d** the maximum dispersion radius of the alien seeds. Here, the linear length of lattices used is $L = 256$, the data correspond to averages over 5,000 independent samples, and to a total evolution time of 6×10^3 MCS

function of the phytotoxic threshold and the maximum dispersion radius of the alien seeds, respectively.

Typical evolutions in time of native plant populations in successful invasions are shown in Fig. 2. The fastest decrease of this population occurs when the native community is homogeneous and constituted entirely of plants with a low resistance to the alien phytotoxin. The slowest decay of the native population occurs in heterogeneous communities with resistant plants distributed at patches in the habitat.

Since the initial condition used in the present simulations corresponds to a disturbed state (seed banks absent in the landscape at the beginning of the invasion), it is relevant to investigate how the

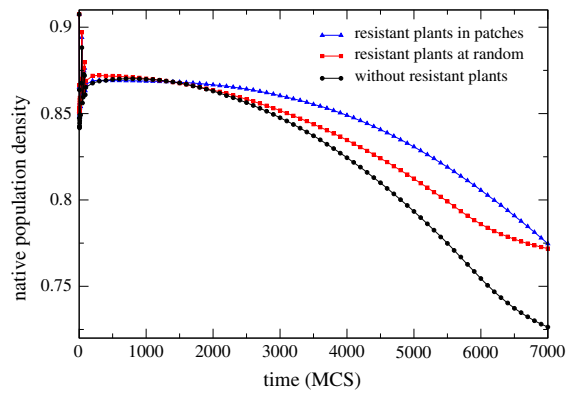

Fig. 2 Evolution over time of native plant populations in successful invasions. The data correspond to averages over 200 independent samples

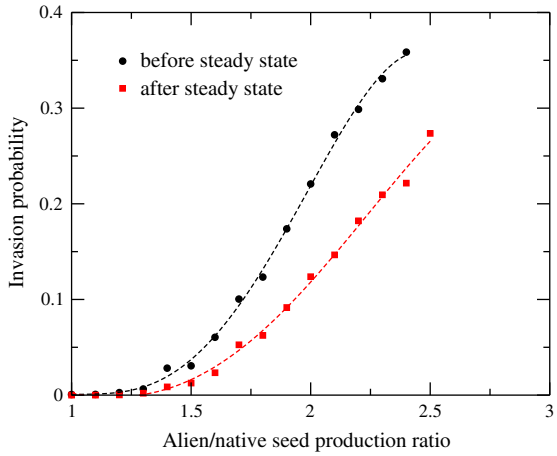

Fig. 3 Invasion probability as a function of the ratio between the numbers of seeds produced by the invasive and the native plants in a native community at its stationary state, i.e., stationary distributions of native seeds and plant ages. Here, the beginning of the invasion occurs at time $t = 60$, greater than the average time necessary for the native community reaches its stationary state. The linear length of lattices used is $L = 100$, the data correspond to averages over 5,000 independent samples, and to a total evolution time of 10^5 MCS

invasion progress in a undisturbed plant community. Therefore, simulations were performed in which the invader plant was introduced at the central site of the lattice only after the native plant population had reached their stationary distributions of ages and of seeds in space. The results for the invasion probability as a function of the ratio between the seed productions of invasive and native plants are shown in Fig. 3. In this figure, the system evolves while there is at least one invader plant or a alien seed on the lattice for a total time one order of magnitude longer than that fixed in Fig. 1a. Consequently, the critical seed ratio and the probabilities for a successful invasion beyond this critical ratio increased in comparison with their counterparts in Fig. 1a.

In Fig. 4 are shown spatial patterns of invasion at different time steps corresponding to a homogeneous native plant community with low resistance to the phytotoxin secreted by the alien species. These invasion patterns are circular with gyration radii that scale as the square root of the numbers of invader plants N_{inv} and smooth surfaces (Hurst exponent $H = 1$) at the asymptotic limit. In turn, the morphology of the invasion patterns changes if a fraction of the native community exhibits a high resistance to the phytotoxin. Typical invasion patterns for resistant plants initially distributed in patches on the native habitat are shown in Fig. 5. It can be noticed that the invasion patterns lost the radial symmetry, yet their gyration radii scale again as $N_{inv}^{1/2}$. However, the border of the invaded region is rough and characterized by a Hurst exponent $H < 0.5$. In addition, as shown in Fig. 6, the spatial patterns of resistant plants also change over time, exhibiting large patches near the invasion front and an exponential decay of their cluster size distributions.

In all the simulations, the gyration radius of the invasion pattern increased linearly in time, as shown in Fig. 7, and thus the invasion speed is constant. The speed of invasion is significantly lower only in the case of resistant plants initially distributed in patches. Furthermore, a rim of empty sites is established adjacent to the invasion front, as seen in Figs. 4 and 5. So, the invasion progress by suppressing the native plants near its expanding border.

Discussion

The complexity and diversity of the phenomena underlying plant invasions, the range of spatial and temporal scales over which they act, extending from the molecular to the ecological levels, and the intricate way in which they are interwoven, make it nearly impossible to understand biological invasions based on intuition alone. The development of quantitative theoretical models for plant invasions, such as the one presented here, might be a very useful approach to deduce how distinct mechanisms interact in invasion processes. It also allows to integrate the rapidly increasing amount of information obtained at the various scales in accurate models, and to predict the macroscopic response of the system to control interventions. Such mechanistic models can provide insights into critical traits that control invasion success and also guide the design of new assays by indicating relevant processes for further investigation. In addition, mathematical modeling can prevent excessive experimentation needed to develop effective control strategies.

The present model demonstrates that seed production and dispersal distance, both traits associated to the invader species, as well as the native susceptibility to the alien phytotoxin determine the success probability and the invasion speed. A greater seed

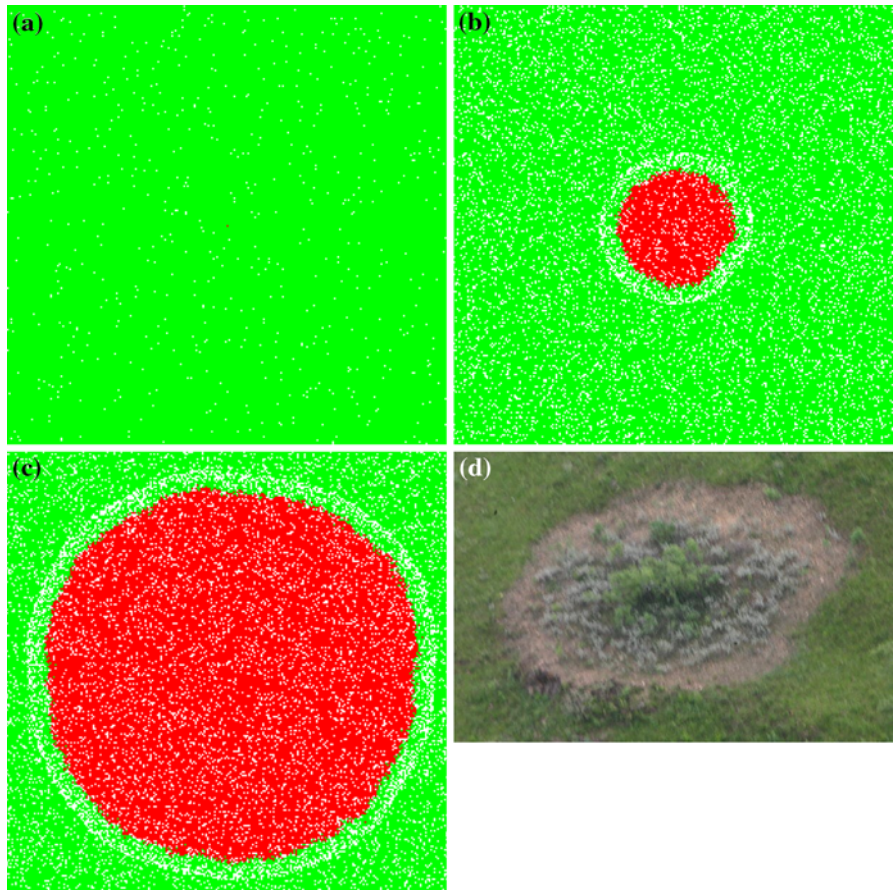

Fig. 4 Spatial patterns of a typical invasion in a homogeneous native plant community with low resistance to the phytotoxin secreted by the alien plant. Three different time steps **a** $t = 1$, **b** $t = 1{,}000$, and **c** $t = 3{,}000$ are shown. *Light gray*, *gray* and *white* pixels correspond to native plants, invader plants and empty sites, respectively. Again, $L = 256$ was used. The invasion patterns should be compared with the one shown in **d** for the *Vochysia* sp. (*Vochysiaceae*), in Brazil

production by the alien species is necessary for the invasion success and a higher native sensitivity to its phytotoxin enhances this success. Indeed, the chance of the invader plant to colonize new sites increases due to a larger alien seed bank present at this site coupled with a decreased germination probability of the local native seeds. Also, the greater death rate of the native juveniles affected by the invader phytotoxin further enhances the displacement of the native plants. However, a long-range dispersal of the invasive seeds has an opposite effect, since their seed banks nearby the already invaded area decrease. But it is just on the edge of the invaded region, where a greater phytotoxin concentration strongly impairs native seed germination and seedling establishment, that the colonization opportunities occur.

It is worth to emphasize the main role of disturbances in influencing invasive success. In our simulations, the evolution in time of the plant community starts from an initial state without seed banks everywhere at the onset of invasion. Such a disturbance can be interpreted as a fire that burns the seeds of the native plants on the soil. This "fire" enhances the establishment rate of invasive plants, as shown in Fig. 3. Indeed, the invasion probability decreases significantly in a native community that already has reached its stationary spatial distribution of seeds. However, as is the case in the present model, invasion occurs even in natural communities without disturbance, at least for allelopathic invaders (1) exuding phytotoxins with large and multiple effects on the native plants and (2) having a higher rate of seed production. So, the model demonstrates that these two conditions are sufficient for a successful allelopathic invasion. But, are they necessary conditions? Does an invasion occurs if the phytotoxin affects some, but not all, traits (seed germination, seedling establishment, adult mortality and fertility) of the native plants? Also, does the

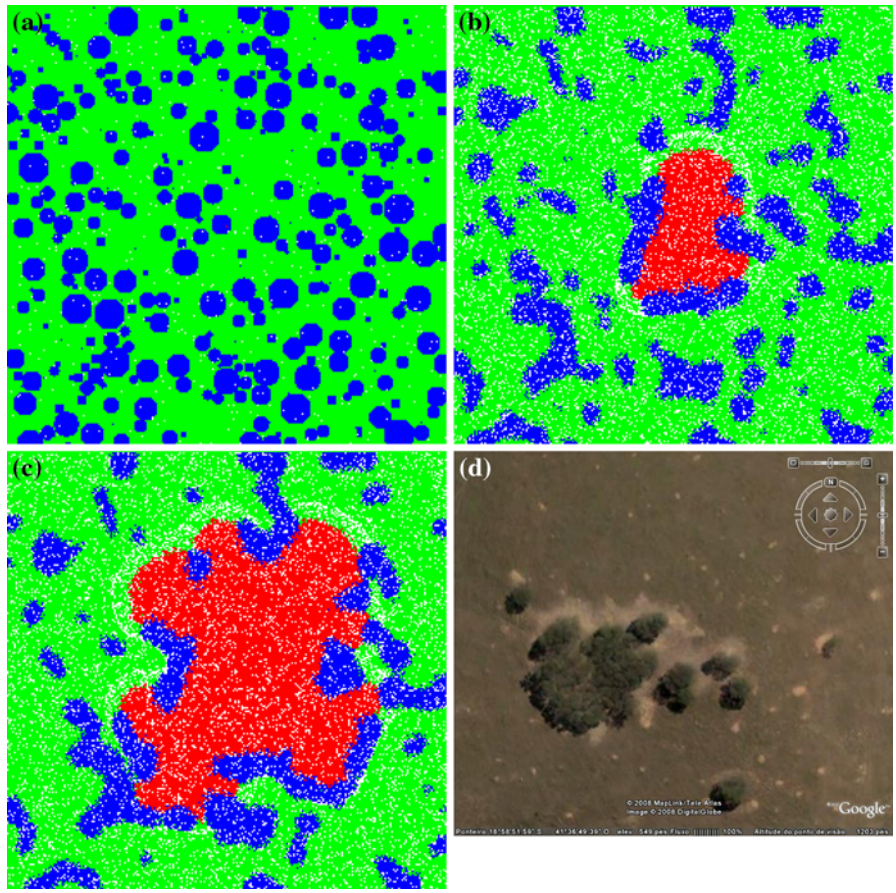

Fig. 5 Spatial patterns of a typical invasion in a heterogeneous native community with high resistant plants distributed in patches. Three different time steps **a** $t = 1$, **b** $t = 1{,}500$, and **c** $t = 3{,}000$ are shown. For comparison, an invasion pattern of *Myracrodruon urundeuva* (*Anacardaceae*) in Brazil is shown in **d**. *Light gray*, *black*, *gray* and *white* pixels correspond to native plants, native resistant plants, invader plants and empty sites, respectively. Again, $L = 256$ was used

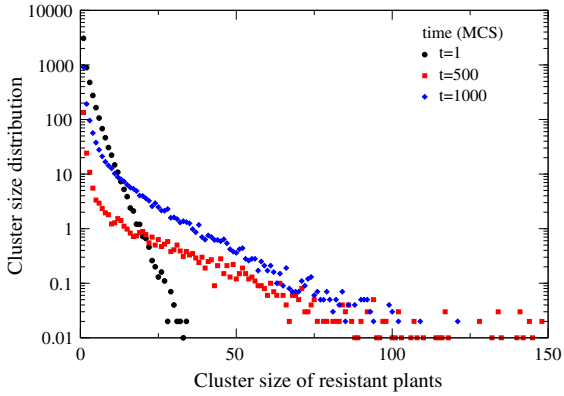

Fig. 6 Time evolution of the cluster size distributions of resistant native plant. The initial patches, randomly dispersed in the habitat, were compact, round and exponentially distributed in size with a characteristic size $n_s(0) = 7$. The data correspond to an average over 200 independent samples

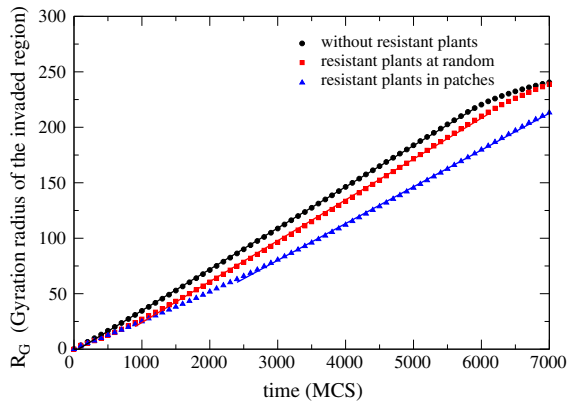

Fig. 7 Time evolution of the gyration radius of the invaded region. The invasion speeds are 0.0372, 0.0368, and 0.033 lattice constant per MCS in the case of native plants with low resistance to the phytotoxin, heterogeneous native community with high resistant plants distributed at random, and in patches, respectively. Again, the data correspond to an average over 200 independent samples

invasion occurs if there are distinct phytotoxic thresholds for each one of the native traits? These issues will be addressed in a future work.

The patterns of invasion shown in Figs. 4 and 5 range from circular with smooth fronts (Hurst exponent $H = 1$), in a homogeneous native community, to irregular shapes with rough fronts ($H \neq 1$), in a heterogeneous native community containing resistant plants. Such patterns are, for instance, qualitatively very similar to the invasion patterns of *Vochysia* sp. (*Vochysiaceae*) (Fig. 4d) and *Myracrodruon urundeuva* (*Anacardaceae*) (Fig. 5d), in Brazil. This naive comparison suggests that the variety of patterns generated by the present model is able to represent the range of shapes associated to the allelopathic spreading of invasive plants with short-distance seed dispersal. Indeed, initial patterns distinct from the single seed used in our simulations will certainly lead to spatial structures more similar to the patterns of allelopathic invasion observed in nature. Even branched or dendritic invasion patterns are possible in a heterogeneous environment in which, for example, the phytotoxin's diffusivity exhibits a spatial variation. Moreover, the auto-toxic effects of the phytotoxin on the invader, a relevant biological feature neglected in the present model, will probably constitute a long-range inhibitory mechanism necessary for the emergence of complex Turing-like patterns.

From a different perspective, the spatio-temporal patterns generated by models for plant invasion exhibit remarkable similarities with cancer progression either in the case of long- or short-distance seed dispersal (Hu et al. 2003; see Fig. 3a, b in this reference). The patterns of plant invasions mediated by invader-secreted phytotoxins shown in Figs. 4 and 5 exhibit neat borders surrounded by rims of empty sites into which the invasion fronts expand. Allelochemicals destroy the native community at the border of the invaded area as matrix metalloproteases (Hu et al. 2003) and lactic acid (Gatenby and Gillies 2004) disrupt the extracellular matrix adjacent to a primary tumor. Likewise low or non-invasive tumors, in which cancer cells have a reduced migration, the short-distance dispersion of the invader seeds generates a defined invasion front.

Concerning population heterogeneity, the inclusion of naturally more resistant native plants to the invader phytotoxins did not lead to a failure of the invasion processes, but decreased their probabilities of success and lowered the invasion velocities. Moreover, the invasion front can be locally pinned by the resistant native plants, but eventually advances in between the blocked areas, as shown in Fig. 8. In the case of resistant plants distributed at random, the gyration radius of the invaded region grows linearly in time and the asymptotic roughness exponent is $H \sim 0.76$. Hence, due to the random pinning the invasion front becomes rough. Because all the pinning forces are eventually overcome, the present model for plant invasion seems to be closely related to the Zhang non-Gaussian noise model (Zhang 1990) for which a Hurst exponent $H \sim 0.75$ was obtained for $\mu = 3$. There, the exponent μ controls the power law distribution of the noise $\eta(i, t)$ (that is, $P(\eta) \sim \eta^{-(1+\mu)}$ if $\eta > 1$, or $P(\eta) = 0$, $\eta \leq 1$). However, in contrast to Zhang's model, in the present cellular automata the pinning field fluctuates in time due to the death and birth (colonization/establishment) of native resistant plants. Therefore, it is not clear if the plant invasion process considered here can be formulated in terms of the Zhang's model, or even why an exponent $\mu = 3$ should be expected. In turn, a distribution in patches of the resistant native plants further increases the roughness of the invasive front. Also, the corresponding invasion patterns suggest that if the driving field (phytotoxin concentration) is sufficiently weak compared to the random resistance field strength (phytotoxic threshold θ), the front will be stuck and the invasion area will be frozen. This can be the case if, for instance, an auto-toxic effect of the allelochemicals on the invader plant itself is considered. In the large driving force/late time regime, a value of about $0.25 = 1/4$ for the surface width growth exponent β was found for interface growth process governed by the quenched disorder Edward–Wilkinson equation (Meakin 1998). Again, it is not clear what the appropriate continuum limit equation may be to describe the invasion process considered here. Anyhow, in terms of the growth of a driven interface, a successful invasion can occur only above the depinning transition. From a biological point of view, this is an interesting concept which brings into focus the ecological factors that possibly determine the pinning–depinning threshold. Interfering in such factors in order to pin the invasion front might be an effective control strategy for biological invasions.

The extreme effects of invaders on native populations have the potential to select and drive further

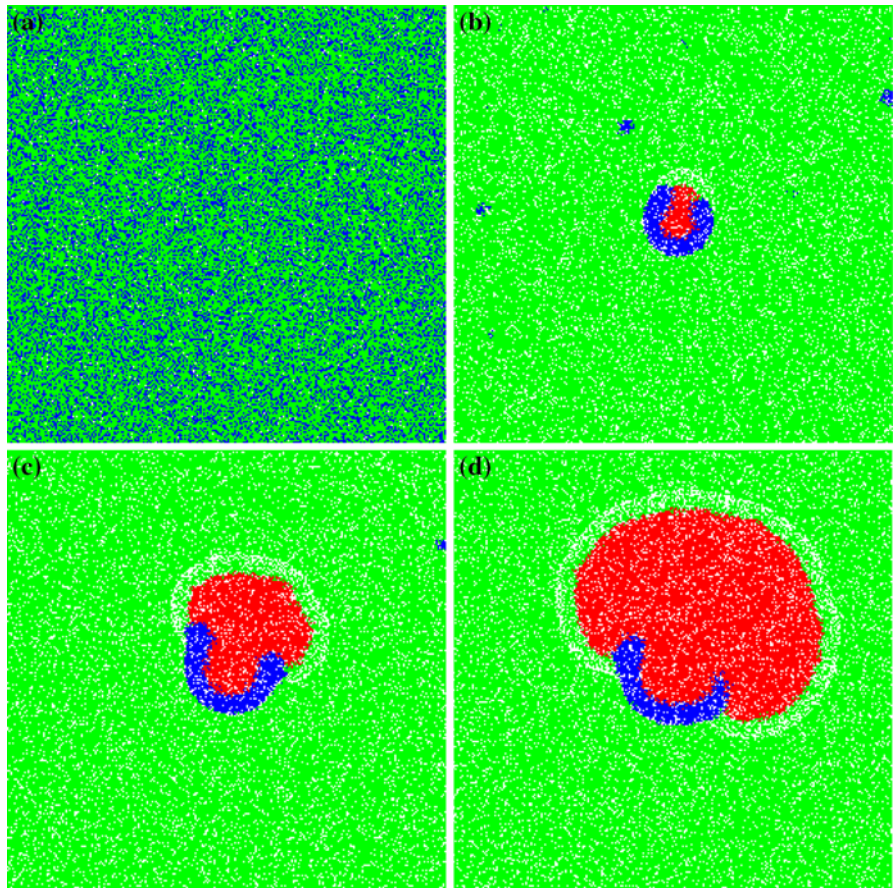

Fig. 8 Spatial patterns of a invasion process locally pinned by the presence of native plants resistant to the phytotoxin secreted by the alien plant. Four different time steps **a** $t = 0$, **b** $t = 1{,}000$, **c** $t = 2{,}000$, and **d** $t = 3{,}000$ are shown. *Light gray*, *black*, *gray* and *white* pixels correspond to native plants, native resistant, invader plants and empty sites, respectively. Again, $L = 256$ was used

adaptation of native resistant species. Therefore, if the resistant plants generated by natural genotypic variations inside the native plant community can be rapidly selected by the particular rhizosphere chemistry of the invader, invaded communities may recover some aspects of their natural structure and function, and invaders and natives may eventually coexist. This can be achieved, for instance, through the increase of native phytotoxic threshold θ, assumed fixed and high in the present model, or specially if auto-toxic effects on the invader plant are included in the model. It is worth mentioning that experiments performed by Callaway et al. (2005) demonstrated a wide variability in the resistance of native grasses to (±)-catechin phytotoxin secreted by the invader *C. maculosa*. Furthermore, Mealor et al. (2005) found out that populations of perennial grasses exposed to long-term coexistence with *Acroptilon repens* differed genetically from those at adjacent non-invaded patches.

Conclusions

A multiscale model has been proposed to study alien plant spread mediated by allelopathic suppression. It assumes a homogeneous habitat, density-dependent growth and interspecific competition for resources between native and alien species. The probability of a successful invasion, the corresponding spatial patterns and their evolution in time, characterized in terms of population curves, gyration radii of the invaded regions and their interface roughness, were analyzed.

The main results are: in addition to the phytotoxin nature (synthesis and degradation rates, diffusivity and phytotoxic threshold), invasive patterns and invasion success depend on the composition of native plants in the area. In fact, both success and invasion speed decrease in the presence of resistant native plants. Also, self-affine invasion fronts are smooth (Hurst exponent $H = 1$) in the absence of resistant

plants, but rough ($H \neq 1$) on the contrary. Moreover, if the resistant native species is randomly distributed on the landscape, the invasion front exhibits long-range correlations ($H \sim 0.76$), while this border is anti-correlated ($H \sim 0.20$) if resistant plants are distributed in patches. Finally, the cluster size distribution functions of resistant plants are exponentials with characteristic cluster sizes increasing in time.

Acknowledgments The authors would like to thank an anonymous referee for calling our attention to the effects of a disturbed initial state on the invasion process and for other valuable suggestions that improved the paper. Special thanks are due to Professor Alvaro Neves (UFV, Brazil) for the final editing of the manuscript. This research was partially supported by the Brazilian agencies CNPq, CAPES and FAPEMIG.

References

An M, Pratley JE, Haig T (1996) Applications of GC/MS in allelopaty research: a case study. Rapid Commun Mass Spectrom 10:104–105

Bais HP, Walker TS, Stermitz FR et al (2002) Enantiometric-dependent phytotoxic and antimicrobial activity of (±)-catechin. A rhizosecreted racemic mixture from spotted knapweed. Plant Physiol 128:1173–1179

Bais HP, Vepachedu R, Gilroy S et al (2003) Allelopathy and exotic plant invasion: From molecules and genes to species interactions. Science 301:1377–1380

Bais HP, Park SR, Weir TL et al (2004) How plants communicate using the underground information superhighway. Trends Plant Sci 9:26–32

Barabási A L, Stanley HE (1995) Fractal concepts in surface growth. Cambridge University Press, Cambridge

Callaway RM, Aschehoug ET (2000) Invasive plants versus their new and old neighbors: a mechanism for exotic invasion. Science 290:521–523

Callaway RM, Ridenour WM, Laboski T et al (2005) Natural selection for resistance to the allelopathic effects of invasive plants. J Ecol 93:576–583

Cannas SA, Marco DE, Páez SA (2003) Modelling biological invasions: species traits, species interactions, and habitat heterogeneity. Math Biosci 183:93–110

Chou C (1999) Roles of allelopathy in plant biodiversity and sustainable agriculture. Crit Rev Plant Sci 18(5):609–636

Crawley MJ (1996) Biodiversity. In: Crawley MJ (eds) Plant ecology, 2nd edn. Blackwell Science, London, pp 595–632

Dale PJ, Clark B, Fontes EMG (2002) Potential for the environmental impact of transgenic crops. Nature Biotechnol 20:567–574

Dean WRJ (1998) Space invaders: modeling the distribution, impacts and control of alien organisms. Trend Ecol Evol 13:256–258

Drake JA, Mooney HA, di Castri F et al (eds) (1989) Biological invasions: a global perspective. Wiley, Chichester

Ermentrout GB, Edelstein-Keshet L (1993) Cellular automata approaches to biological modeling. J Theor Biol 160:97–133

Gatenby RA, Gillies RJ (2004) Why do cancers have a high aerobic glycolysis? Nat Rev Cancer 4(11):891–899

Glimm J, Sharp DH (1997) Multiscale science. a challange for the twenty-first century. SIAM News 30:4, 17, 19

Hu B, Guo P, Fang Q et al (2003) Angiopoietin-2 induces human glioma invasion through the activation of matrix metalloprotease-2. Proc Natl Acad Sci USA 100:8904–8909

Keddy PA (1989) Competition. Chapman and Hall, London

Krumhansl JA (2000) Multiscale science: materials in the 21st century. Mater Sci Forum 327(8):1–8

Martins ML, Ferreira SC Jr, Vilela MJ (2007) Multiscale models for the growth of avascular tumors. Phys Life Rev 4:128–156

Meakin P (1998) Fractals, scaling and growth far from equilibrium. Cambridge University Press, Cambridge

Mealor BA, Hild AL, Shaw NL (2005) Native plant community composition and genetic diversity associated with long-term weed invasions. West North Am Nat 64:503–513

Perry LG, Thelen GC, Ridenour WM et al (2005) Dual role for an allelochemical: (±)-catechin from *Centaurea maculosa* root exudates regulates conspecific seedling establishment. J Ecol 93:1126–1135

Petrovskii S, Shigesada N (2001) Some exact solutions of a generalized Fisher equation related to the problem of biological invasion. Math Biosci 172:73–94

Rice EL (1984) Allelopathy, 3rd edn. Academic Press, London

Sherratt JA, Lewis MA, Fowler AC (1995) Ecological chaos in the wake of invasion. Proc Natl Acad Sci USA 92:2524-2528

Shigesada N, Kawasaki K, Teramoto E (1986) Traveling periodic waves in heterogeneous environments. Theor Popul Biol 30:143–160

Shigesada N, Kawasaki K (1997) Biological invasions: theory and practice. Oxford University Press, Oxford

Silva HS, Martins ML, Vilela MJ et al (2006) 1/f ruffle oscillations in plasma membrane of amphibian epithelial cells under normal and inverted gravitational orientations. Phys Rev E 74:041903

Snow AA (2002) Transgenic crops—why gene flow matters. Nat Biotechnol 20:542

Varnijic JA, Wood MJ, Barnard J (2000) Soil-mediated effects on germination and seedling growth of coastal wattle (*Acacia sophorae*) by the environment weed, biton busy (*Chrysanthemoides monilifera* spp. *Rotundata*). Austral Ecol 25:445–453

Walker LR, Vitousek PM (1991) An invader alters germination and growth of a native dominant tree in Hawaii. Ecology 72:1449–1455

Weir TF, Bais HP, Vivanco JM (2003) Intraspecific and interspecific interactions mediated by a phytotoxin, (−)-cathechin, secreted by the roots of *Centaurea maculosa* (SPOTTED KNAPWEED). J Chem Ecol 29:2397–2412

Wolfram S (1986) Theory and application of cellular automata. World Scientific, Singapore

Zhang YC (1990) Non-universal roughening of kinetic self-affine interfaces. J Phys 51:2129–2134